

Deployment Mechanisms for High Packing Efficiency One-Meter Reflectarray Antenna (OMERA)

Jonathan F. Sauder¹, Manan Arya², Nacer Chahat³, Ellen Thiel⁴, Sean Dunphy⁵,
Mengjan Shi⁶, Greg Agnes⁷, Tom Cwik⁸

Jet Propulsion Laboratory, California Institute of Technology, Pasadena, CA, 91109

While the capabilities of CubeSats have greatly increased in the past years, large, deployable high frequency apertures remain a limitation. The goal of this work is to develop a large 1 meter antenna operating at 35.75 GHz for RADAR applications. A reflectarray design was selected, as the flat panels are compatible with the CubeSat form factor. A center-fed, Cassegrain configuration was selected for the feed, to minimize deployed height. The flat panel configuration and Cassegrain feed allowed the entire 1 meter antenna to be compatible with a 6U bus, leaving a little under 4U of volume for remaining instrument and spacecraft components. Several iterations of the design have been built and tested, with an RF test of a fully deployed assembly being completed most recently. Prior to constructing the flight model, another iteration will need to be built and tested. The goal is to have the antenna flight ready before 2020.

I. Introduction

The opportunities for CubeSats seem endless, as technology and launch opportunities for CubeSats have greatly increased in the past years. This enables a greater variety of missions, including opportunities for missions beyond low earth orbit. As operational distances between CubeSats and Earth increases and instruments become more advanced, data rates and instrument aperture become limiting factors. The need to improve these capabilities can be witnessed by programs like the CubeQuest Centennial Challenge¹, in which NASA is seeking innovative solutions to improve data rates. Currently, many CubeSats communicate on UHF bands, and those utilizing S-band or X-band patch antennas are considered to have high data rates. Some instruments focus on arrays of patch antennas as well. However, these will not achieve the high data rates or large apertures/high frequencies required for more advanced instruments and interplanetary data communications. A compelling solution can be found by designing a deployable antenna operating at the high, Ka-band frequency which improves gain by 3 to 4 or more orders of magnitude.



Figure 1: OMERAs As Built

¹ Mechatronics Engineer, Technology Infusion, 299-101, 4800 Oak Grove Drive, Pasadena, CA, AIAA Member

² Technologist, Deployable Structures, 299-101, 4800 Oak Grove Drive, Pasadena, CA, AIAA Member

³ RF Engineer, Spacecraft Antennas, 161-260, 4800 Oak Grove Drive, Pasadena, CA

⁴ Mechanical Engineer, Payload Development, 303-400, 4800 Oak Grove Drive, Pasadena, CA

⁵ Mechanical Engineering Intern, Technology Infusion, 299-101, 4800 Oak Grove Drive, Pasadena, CA

⁶ Mechanical Engineering Intern, Deployable Structures, 299-101, 4800 Oak Grove Drive, Pasadena

⁷ Senior Mechanical Engineer, Deployable Structures, 299-101, 4800 Oak Grove Drive, Pasadena, CA, AIAA Member

⁸ Manager, Space Tech Office, 180-700, 4800 Oak Grove Drive, Pasadena, CA

II. Background

Deployable antenna concepts can be organized by architecture, each of which have strengths and weaknesses in meeting CubeSat communication and science needs. Architectures include solid deploying reflectors, shape memory reflectors, inflatables, reflectarrays, and mesh reflectors. Solid deploying reflectors have great surface accuracy, but do not stow well in small spaces and can be heavy (e.g. Hughes spring-back antenna²). Shape memory reflectors may work at lower frequencies, but much development is still required as, at Ka-band, the surface is not accurate enough³. Inflatable reflectors⁴ stow well and are lightweight, but have issues with maintaining inflation and shape.

The remaining two architectures, parabolic antennas and reflectarrays are the most attractive for high frequency, large aperture antennas on a CubeSat. Parabolic reflectors utilize a parabolic shape to focus RF energy to a focal point. Parabolic reflectors developed for CubeSats have included goer-wrap composite reflector⁵, the Aeneas 0.5 meter S-band antenna⁶, a very thin ribbed, wrap rib design⁶, the 0.5 meter Ka-band Parabolic Deployable Antenna (KaPDA)⁷, and the 1.0 meter Ka-band KaTENna. While parabolic antennas work well at a number of frequencies, they generally present a more challenging approach for deployment, as a curved parabolic surface is required. Also, parabolic reflectors tend to be labor intensive to build.

The reflectarray operates by using individual patches, arranged to provide a progressive reflection phase shift across the antenna surface, to generate a plane wavefront. This enables a flat surface to behave, at least from an RF point of view, like a parabolic surface. The key disadvantage of reflectarrays is that they can only work at their designed frequencies. However, often this is offset by the advantages; a flat surface is easier to deploy, packs more efficiently when stowed, and tends to be less challenging to build.

The first reflectarray to fly in space was on the CubeSat ISARA⁸ (Integrated Solar Array and Reflectarray Antenna). This was a 0.3 meter by 0.3 meter Ka-band antenna. One of the key advantages of using a reflectarray on the CubeSat, is that the reflectarray can be stored in the “bonus” space on a CubeSat, allocated for the solar panels, minimizing the impact the antenna has on usable volume. The next reflectarray design developed for the CubeSat form factor was Mars Cube One⁹ (MarCO), which doubled the size of the deployed reflectarray to 0.3 meters by 0.6 meters. The frequency however dropped from Ka-band to X-band, as it was being used as a telecommunications relay for the Insight lander.

OMERA takes the MarCO concept to the next level, by quadrupling the size and increasing the frequency an order of magnitude from X-band to Ka-band. This has profound implications on the design, as it means the surface accuracy requirements increase by nearly an order of magnitude. The larger size means there are many additional hinges and deployment mechanisms. But, both of these scope growths increase antenna capability, which can best be represented by gain, going from 29.2 dB for MarCO to 48.1 dB for OMERa.

III. RF Design

The RF optical design drives the rest of the antenna design, as well as the requirements on the mechanical shape. A deployable antenna requires close collaboration between RF and mechanical engineers to ensure the design is realistic from both perspectives. The first RF trade to be completed was determining if a center fed design or an offset fed design would be used. The offset fed design would be similar to the ISARA and MarCO reflectarrays, and the feed would be located on one side of the CubeSat, with the reflectarray panels on the other. The offset fed design is advantageous as the feed does not need to deploy as far, and multiple feeds can use the same reflector if desired. However, there are disadvantages due to blockage of the reflectarray by the CubeSat body and deployment errors are more challenging to control, as an offset design would result in a greater number of hinge lines from the panels to the CubeSat base structure.

The other alternative, a center fed design, placed the feed in the middle of the reflectarray. The key advantage is that it minimized RF losses. However, the feed must be deployed a significant distance in the center of the reflectarray antenna. The configuration is shown in Figure 1.

To minimize the requirements on deployed height of the feed, a Cassegrain configuration was used, as it places the secondary reflector for the feed below the focal point of the antenna. Even this reduced distance required the sub-reflector to deploy 0.62 meters, and the horn to deploy 0.48 meters out of the CubeSat body. Once the depth inside the CubeSat body to store the feed was considered, the total deployment distance was 0.82 meters. Utilizing a Cassegrain design also enabled the reuse of a design similar to the Ka-band Parabolic Deployable Antenna feed¹⁰, which resulted in quicker development of the concept. A similar telescopic approach was taken to the waveguide. But now, instead of just the horn telescoping around the waveguide, two sections of waveguide and the horn telescope, resulting in a 3 element telescopic design.

Because of this new multi-element telescoping design and novel nature of reflectarrays, it was critical to test a non-deployable antenna to verify the RF design early. A non-deploying reflectarray, along with a non-deploying feed (but with variations in diameter of the waveguide to simulate the telescoping nature of the waveguide) was tested to verify RF performance, and found to achieve 48.1 dBi of gain. As the performance aligned with the simulations, this enable continuation of the mechanical design for the antenna. The description of the mechanical design is divided into two sections, to fit two key components: the deployable feed and the deployable panels.

IV. Mechanical Design: Deployable Feed

The mechanical requirements on the feed were to stow in a 200 mm height, consume less than a 2U volume, deploy with an accuracy of 0.4 mm in all directions, and accommodate a 3 part telescoping waveguide. The waveguide transitions had to be located at specific points along that waveguide to ensure integrity of the RF signal.

To fit within the compact volume, the best approach to control feed location was cables. The cable length could be precisely adjusted to hold the feed in the correct location. The feed would be preloaded against the cables with a spring. While originally the focus was to keep the cables in the center to minimize the footprint it was quickly realized while this controlled height (Z direction in Figure 1) of the feed precisely, it did not control the horizontal position (or X and Y) accurately enough. It was necessary to provide the cable with a longer moment arm, which was accomplished by moving the attachment points out to the edge of the CubeSat Body. This provided much more precise positioning of the feed in the horizontal plane.

A. Initial Dynamic Deployment Design

The goal of the first feed deployment design was to keep it as simple as possible by utilizing compression springs. Two compression springs were used; one deployed the sub-reflector, telescoping it along the feed, and another deployed the feed horn. This design was essentially an extension of the KaPDA deployment for the sub-reflector. While the long spring designed to deploy the feed was buckled when fully deployed due to its long length, this was deemed as acceptable as the waveguide prevented the spring from buckling too far out of plane (See Figure 3, right). Utilizing two springs increased the amount of preload and decreased the amount of kinetic energy requiring dissipation at the end of deployment. Further, to assist with additional energy dissipation, the cables setting the height of the feed were attached to stiff, preloaded springs, creating shocks absorbers.

However, despite utilizing two separate springs and adding energy absorbing shocks, deploying 0.82 meters under the power of a compression spring resulted in an extremely dynamic deployment. This initial design had enough energy at the end of deployment that it caused the entire CubeSat chassis, and GSE, to leap into the air by several inches, and thus required the addition of two 45 lbs weights to keep the chassis fixed during deployment. At the same time, the preload and tension in the cables was so low when deployed, that the deployed feed was in constant motion due to the air conditioning. To increase preload in the spring would only also increase energy from the deployment. Therefore, the design did not close and a new deployment architecture was required.

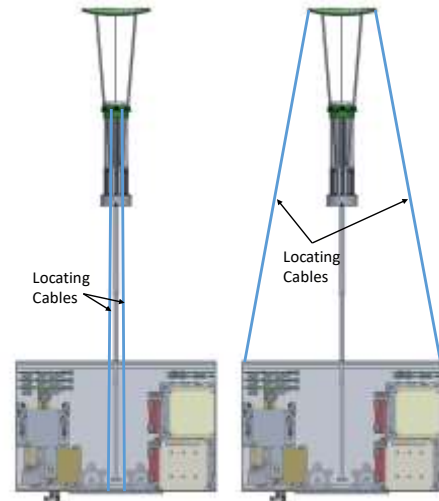


Figure 2: Center (left) vs. edge (right) attached locating cables

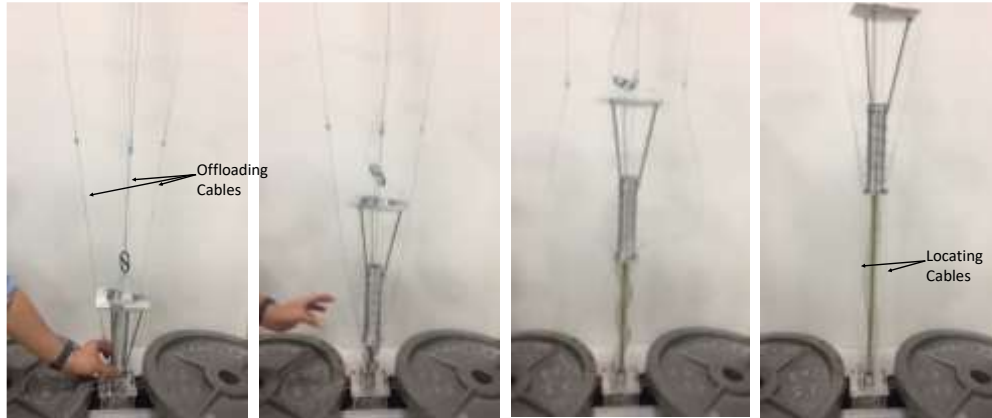


Figure 3: Deployment with a Spring Powered Design

B. Controlled, Deterministic Deployment

To increase the amount of preload in the deployed state, and to decrease the amount of energy in the deployment, alternate deployment methods were explored. Initially, a telescoping structure, powered by a looped cable running through a series of pulleys was investigated. However, due to the tight volume constraints within the CubeSat, the “large” size of the telescoping structure, and the required cable pulley minimum diameter, this configuration was abandoned.

The second configuration explored was a deployment mechanism using tape measures. Two tape measures were attached to the sub-reflector collar, one on either side. As the tape measures were unrolled, they would push up the sub-reflector collar causing the sub-reflector to telescope along the horn, and then the horn to telescope along the waveguide. The deployed position of the feed was controlled by a quartz cable hexapod. Initial analysis indicated the structure would support itself under gravity, so that gravity offloading could be avoided.

An early prototype was built, where each tape was attached to a spool which was attached to a hand crank. While the design was rough, it proved the deployment mechanism worked, and that approximately 6 lbs of upward force could be used to deploy the tapes. However, it was very challenging to keep the two tapes in sync with each other, and just a few tenths of an inch of asynchronous motion caused the entire assembly to tilt to one side and would overpower the positioning ability of the cables. Positional tolerances were not close to being met. It was realized that during a mission, the two tapes could be at different temperatures, which would result in differential thermal expansion and introduce error into the tape position.

To improve on this design, two changes were made. First, a motorized tape deployer was procured from Tendeg, to ensure both tapes would deploy synchronously. While the deployer was motorized, it was noticed when transition

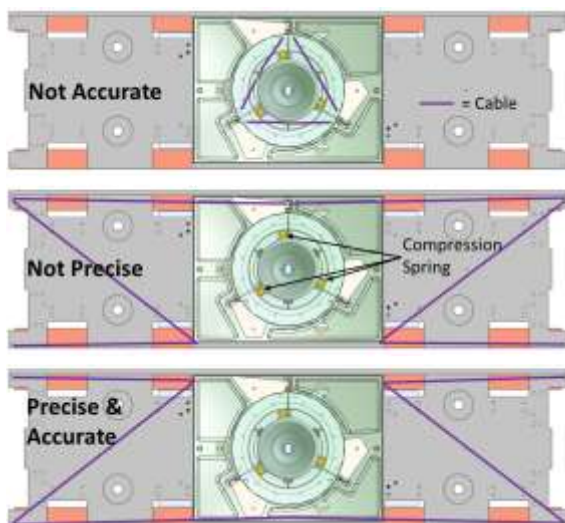


Figure 4: Cable Attachment Approaches

between stowing and deploying, the deployed tape on one side would wind up more than the tape on the other side. While the tapes always returned to the same position in the stowed and deployed state, there was hysteresis in transition between the two, causing the sub-reflector to tilt between the stowed and deployed conditions. This hysteresis was due to variability in how the tape wound around the spool and friction inside the deployment mechanism.

The second change was splitting the sub-reflector collar into two parts. One attached to the sub-reflector and positioned the horn, which required precise placement, and the second attached to the tapes. The upper and lower halves of the sub-reflector collar were connected with a set of three compression springs, providing compliance. There was over 3mm of compliance in the vertical Z dimension and about 0.4 mm of compliance in both X and Y horizontal dimensions. This would more effectively decouple the

tapes and positioning cables as the tapes provided an upward force and the cables located the sub-reflector in X, Y, and Z.

The mounting location of the cables relative to the CubeSat bus and the three compression springs on the collars was tested, to explore the effect of cable placement on absolute accuracy and deployment repeatability (or precision). The easiest accommodation was to place the cables at the center of the CubeSat. But, as noted earlier this did not provide enough control authority to position the sub-reflector accurately as the tapes were not precisely on center. By moving the cables to the corner of the CubeSat, the cables had a greater moment arm, and thus had the control authority to pull the tapes into the correct position. Location of the sub-reflector positioning cable attachment points and the three compression springs between the two halves of the sub-reflector collar was also found to be critical. If the cables were placed directly on top of the compression springs, this resulted in an unstable state that did not produce the required repeatability (Figure 4, middle). However, placing the cable position locations out of phase with the compression springs provided a stable system which consistently deployed to the same position (Figure 4, bottom).

To locate the feed in the desired location, the feed was deployed, its position measured, and then the cables were adjusted by turning small screws which adjusted the cable length. However, because of hysteresis, it was required to partially stow and deploy the sub-reflector after making the adjustment to the screws, allowing the cables to go slack. After the partial deployment, the sub-reflector was now located in its new position, and the cables could be adjusted again, until the sub-reflector was within 0.1mm of the required position. It took approximately 30 to 50 cycles to fine tune the sub-reflector from several mm of error, to 0.1 mm. While the feed could mechanically deploy without gravity offloading, gravity offloading was required to achieve the positional accuracy required.

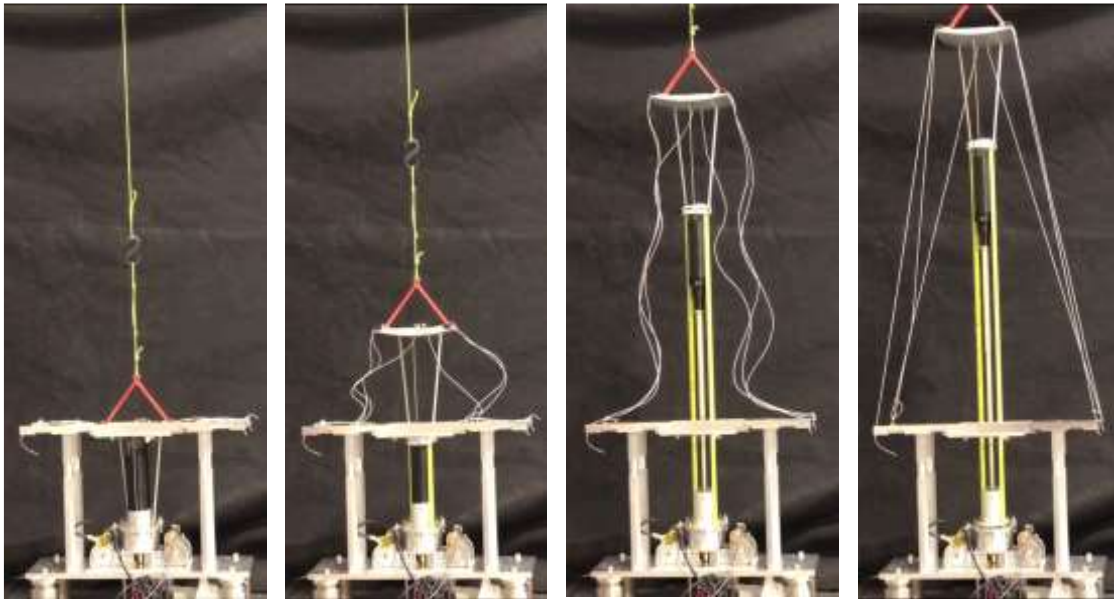


Figure 5: Tape Actuation Provided a more Deterministic Deployment

Initially, knots provided a stopper for the cables in the length adjustment mechanisms. However, knots were very sensitive to which side of the knot was contacting the stopping surface. This meant when getting close to the 0.1 mm alignment, if the cable twisted at all during the partial stow and deployment, the accuracy would be thrown off by up to 0.5 mm. The system became much more robust by replacing the knots with copper crimps which contacted the adjustment mechanism with a flat, uniform surface each time.

V. Mechanical Design: Deployable Panels

Figure 6 shows the deployed OMERA reflectarray. It consists of 16 individual panels, connected by 14 hinge lines. Deployed, the array measures 0.91 m \times 1.05 m, with an area of approximately 0.96 m². The choice of RF frequency and wavelength (35.75 GHz and 8.39 mm, respectively), dictates the desired surface flatness, which is roughly wavelength/20, or about 0.42 mm RMS surface error.

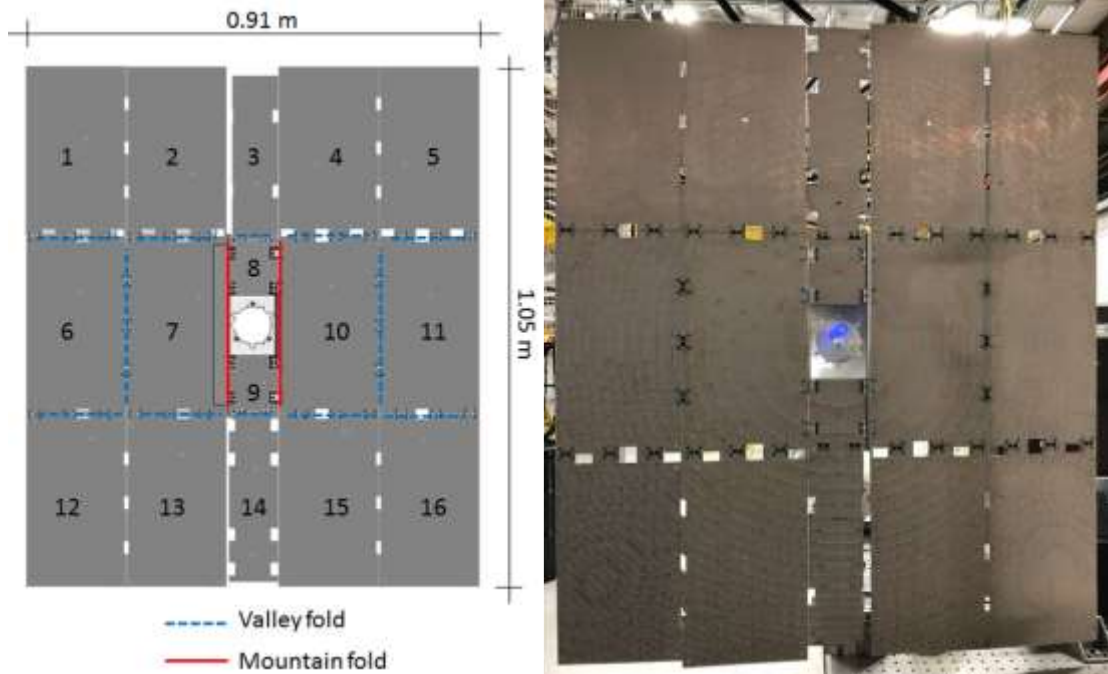


Figure 6: Reflectarray as designed (left) and as built (right)

The 16 panels can be divided into two wings (each consisting of six panels; the left wing consisting of panels 1, 2, 6, 7, 12, 13, and the right wing consisting of panels 4, 5, 10, 11, 15, 16), two side panels (panels 3 and 14), and two body-mounted fixed panels (panels 8 and 9).

The two wings each fold into a stack of six panels against the side of the CubeSat. The two side panels fold atop the stowed feed assembly and fixed panels. The folded configuration of the array is shown in Figure 7. Folded, each wing occupies a volume that is approximately 13 mm × 201 mm × 358 mm on either side of the CubeSat bus, and the folded side panels occupy a volume that is approximately 4 mm × 93 mm × 346 mm atop the CubeSat bus.

Each panel is 2.08 mm thick, consisting of a 1.22 mm (48 mil)-thick STABLCOR composite structural board core, surrounded on both the top and the bottom by a 0.41 mm (16 mil)-thick Rogers 4003 panel, as shown in Figure 8. Each Rogers panel has 17 μm of electrodeposited copper on either side, with the outer copper layer etched to form the reflectarray patches. Only the top Rogers panel is the RF-active reflectarray; the bottom Rogers panel solely provides thermal balance to the panel plate structure.

To achieve the desired surface flatness, this folding architecture required the hinge lines to unfold to a precision of about 0.03 degrees for the body hinges lines (that connect panels 7 and 10 to the CubeSat body), and about 0.1 degrees for the other fold lines. To meet these tolerances, the adjustment capability was designed into the hinges, to allow for the post-assembly measurement and subsequent corrective adjustment of each of the unfolded hinge angles. This decision was reached based on experiments with non-adjustable hinge lines that were unable to meet the needed unfolded angle tolerances.

Most of the hinge lines consist of three separate sprung hinges with the central hinge having a fine-threaded setscrew that allows for



Figure 7: The folded reflectarray. A six-panel-wing is shown folded to the side of the CubeSat body, and the two side panels are shown folded above the CubeSat.

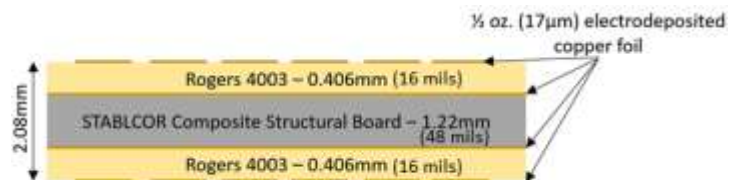


Figure 8: Panel Cross Section

the adjustment of the deployed angle of the hinge line. The exceptions are the body hinge lines (connect panels 7 and 10 to the body of the CubeSat) which comprise four separate hinges with the two central hinges being adjustable in the manner described above; and the side-panel-hinges (connect panels 3 and 14 to the CubeSat body) which comprise two separate hinges, both of which are adjustable.

The adjustable hinge is illustrated in Figure 9. In the unfolded configuration, a fine-threaded ball-end setscrew (with a 200 μm pitch) is pressed against a hard steel insert in the paired hinge leaf (illustrated in green in Figure 8 right). This set screw controls the unfolded angle of this hinge; this angle can be easily and finely adjusted. This allows for the assembly and the bonding of the hinges to the panels to occur with loose tolerances; fine alignment of the array takes place after bonding, by using precision non-contact metrology to measure and then adjust the hinge angles accordingly.

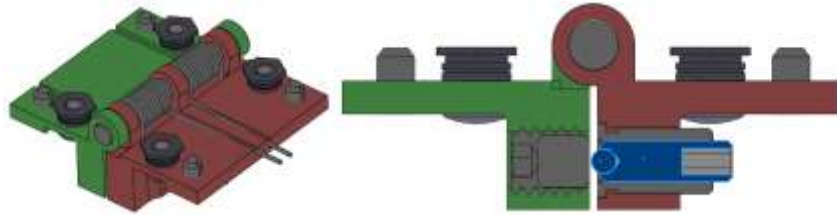


Figure 9: Adjustable hinge design, side view (left) and cross-sectional view (right). The fine-thread set screw is highlighted in blue. Its position can be adjusted with respect to the red hinge to set deployed angle of the hinge

This alignment procedure was used to prepare the deployed reflectarray for RF testing. Figure 10 shows the as-tested surface profile of the reflectarray. The RMS error of 0.345 mm, as tested, was below the typical $\lambda/20$ requirement of 0.42 mm. This measurement was made with a FARO Arm with a Laser Scan head, which has an accuracy of 0.05 mm.

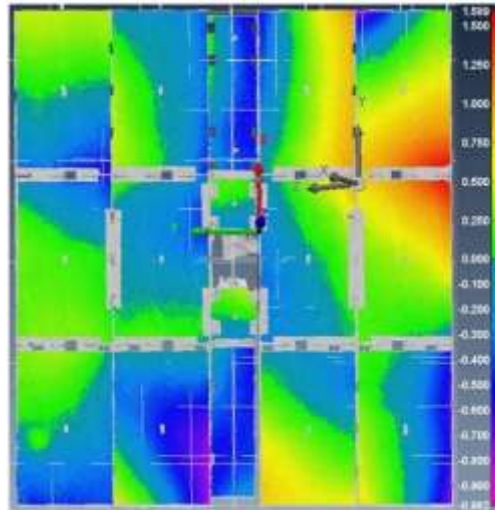


Figure 10: The final adjusted reflectarray surface profile as RF tested. The units on the colorbar are millimeters. The RMS error was 0.345 mm.

VI. Testing of the Feed and Panels

After demonstrating that deployments of both the feed and reflectarray worked mechanically, the next step was to perform deployment repeatability tests. Because of gravity offloading constraints, both the panels and the feed had to be vertical relative to the gravity vector, Z. However, in the combined antenna, the feed and panels are perpendicular to each other. Thus, deployment repeatability testing of the two had to occur in separate tests.

The feed repeatability testing occurred as shown in Figure 5. After the feed was aligned, two deployment tests (three data sets) were run, where the feed was stowed 95% of the way, and then deployed. Deployment repeatability and total error of the deployed feed stayed within 0.25 mm between each of the deployments, which is less than the requirements (Figure 11). On the third deployment, the feed was fully stowed. During the stowing process, a

cracking noise was heard coming from the tapes. The error in absolute accuracy increased to 1.25mm after this deployment. In disassembling the deployment mechanism, it was discovered that the tapes had changed positions slightly by sliding in their attachment to the lower sub-reflector collar resulting in the tapes being located in a different position when deployed. While the connection between the sub-reflector collars had compliance in the vertical direction, there was not enough compliance or clearance in the horizontal direction to accommodate the change in position. Therefore, the approach for attaching the tapes to the sub-reflector collar will need to be modified.

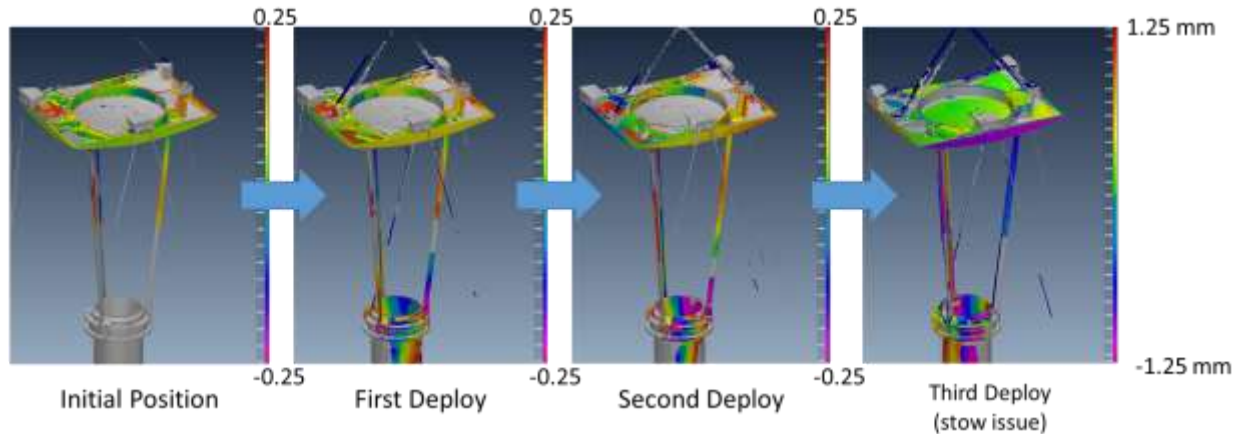


Figure 11: Feed demonstrated deployment repeatability until a full stow.

To show that the designed hinges were capable of achieving the desired accuracy and precision, a series of dynamic deployment tests were done on a testbed of a single wing (comprising 6 panels) of the array. In this testbed (see Figure 12), the panels were made of aluminum sheet, light-weighted to match the weight of the RF-capable panels. This testbed was gravity-offloaded using pulleys and counterweights; each panel was attached at its center of gravity to a cable that was routed over a pulley and connected to a counterweight. This testbed was folded and dynamically deployed 6 times; after each deployment, the hinge angles between the panels were measured using non-contact coordinate measuring.

Figure 13 shows the deviation from 180 degrees in the measured angles after each of the six deployments (Scan ID 2-7), as well as the initial pre-deployed angle (Scan ID 1). The data point is the average of angles calculated from three separate scans of the surface, and the error bar represents the standard deviation. The angle labels reference the designations of the six panels (A1, A2, B1, B2, C1, and C2) as shown in Figure A. The red, green, and blue regions in the plot of Figure B indicate the required deployment tolerance for the hinges; the color of the region corresponds to the color of the plot line for the particular angle. As can be seen, over the six deployments, most of the angles fall within the required regions, indicating excellent accuracy. However, some of the data points lie outside the desired regions; this is because the initial angle of the hinge was not well set. Since the initial hinge angle can be set very finely to be close to 180 degrees, this effect can be avoided. Note that the precision and repeatability of these hinges, which can be calculated as a delta in hinge angle relative to an initial set point, is excellent, as indicated by Figure C, which plots this delta for the six deployments.

After the deployment repeatability was completed, the final step was to perform an RF test. Because of the RF chamber configuration, the feed had to be mounted horizontally and the panels vertically. Because of the limited space in the RF testing chamber and the feed not being mounted in the direction of gravity, both the feed and panel were manually deployed. The panels and feed were then adjusted to have a similar position as was demonstrated in the repeatability tests and gravity offloaded. The FARO laser scan arm was used to determine the position of the components as adjustments were made.

The RF test was successful and demonstrated a similar 48.0 dB gain compared to the original non-deployable design. However, there are still a number of deployments.



Figure 12: Panel Repeatability test with offloading

VII. Conclusions

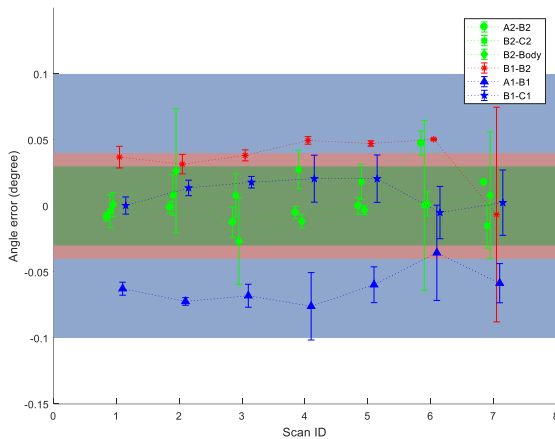


Figure 13: Most panel repeatability results were within the acceptable range, including error bars.

to the stepper motors will not only make deployment easier, but will also improve alignment of the tapes on deployment ensuring both tapes deploy more evenly eliminating the earlier noted hysteresis. Finally, the influence of moving the sub-reflector lower and giving the cables a larger footprint will be explored to see if these changes improve performance.

The panel deployment can also be improved. The panels from the vendor were slightly warped (on the mm scale), but this resulted in stack up errors and is why the panels on the right side had a higher amount of error than those on the left. The first step would be to work with the vendor to develop a method to achieve flatter panels. In parallel, a bonding approach which accommodates greater error can be developed to make the design impervious to panels which are not flat. Finally, the hinges for the prototype were made under a tight deadline, and therefore parts had tolerances of 0.1 mm. However, given extra time, the parts could easily be made within a tolerance of 0.02 mm which would reduce slop in the hinge line and improve panel repeatability.

After making these changes, more deployment repeatability tests will be executed. If these tests find that error has been sufficiently decreased, the next step will be to perform a confirming RF test followed by the flight build. The OMERA is slated to be launched under the Payload Technology Demonstrator (PTD) program with a tentative launch date in 2020.

Acknowledgments

The research was carried out at the Jet Propulsion Laboratory, California Institute of Technology, under a contract with the National Aeronautics and Space Administration. The authors thank Brian Merrill (Spectrum Marine and Model Services), Michel William who assisted in building the antenna, and Dr. Jefferson Harrell who performed the RF tests.

References

- ¹ Mohon, L., "NASA's Cubequest Challenge," NASA Available: http://www.nasa.gov/directorates/spacetechnology/centennial_challenges/cubequest/index.html.
- ² Tan, L. T., and Pellegrino, S., "Stiffening Method for 'Spring-Back' Reflectors," Athens, Greece: ISASR, 2000.
- ³ Bassily, S., and Thomson, M., "Deployable Reflectors," *Handbook of Reflector Antennas and Feed Systems Volume 3: Applications of Reflectors*, Boston, Massachusetts: Artech House, 2013.
- ⁴ Babuscia, A., Corbin, B., Knapp, M., Jensen-Clem, R., Van de Loo, M., and Seager, S., "Inflatable antenna for cubesats: Motivation for development and antenna design," *Acta Astronautica*, vol. 91, Oct. 2013, pp. 322–332.
- ⁵ Reynolds, W., Murphey, T., and Banik, J., "Highly Compact Wrapped-Gore Deployable Reflector," *52nd AIAA/ASME/ASCE/AHS/ASC Structures, Structural Dynamics and Materials Conference*, American Institute of Aeronautics and Astronautics, .
- ⁶ MacGillivray, C. "Scott," "Miniature High Gain Antenna for CubeSats," Apr. 2011.

- ⁷ Sauder, J., Chahat, N., Thomson, M., Hodges, R., Peral, E., and Rahmat-Samii, Y., “Ultra-Compact Ka-Band Parabolic Deployable Antenna for RADAR and Interplanetary CubeSats,” *AIAA/USU Conference on Small Satellites*, Aug. 2015.
- ⁸ Hodges, R., Shah, B., Muthulingham, D., and Freeman, T., “ISARA – Integrated Solar Array and Reflectarray Mission Overview,” *AIAA/USU Conference on Small Satellites*, Aug. 2013.
- ⁹ Hodges, R. E., Chahat, N. E., Hoppe, D. J., and Vacchione, J. D., “The Mars Cube One deployable high gain antenna,” *2016 IEEE International Symposium on Antennas and Propagation (APSURSI)*, 2016, pp. 1533–1534.
- ¹⁰ Chahat, N., Hodges, R. E., Sauder, J., Thomson, M., Peral, E., and Rahmat-Samii, Y., “CubeSat Deployable Ka-Band Mesh Reflector Antenna Development for Earth Science Missions,” *IEEE Transactions on Antennas and Propagation*, vol. 64, Jun. 2016, pp. 2083–2093.